World Academy of Science, Engineering and Technology
International Journal of Biomedical and Biological Engineering
Vol:4, No:1, 2010

An Adaptive Mammographic Image Enhancement in Orthogonal Polynomials Domain

R. Krishnamoorthy, N. Amudhavalli, M.K. Sivakkolunthu

***Abstract*—**X-ray mammography is the most effective method for the early detection of breast diseases. However, the typical diagnostic signs such as microcalcifications and masses are difficult to detect because mammograms are of low-contrast and noisy. In this paper, a new algorithm for image denoising and enhancement in Orthogonal Polynomials Transformation (OPT) is proposed for radiologists to screen mammograms. In this method, a set of OPT edge coefficients are scaled to a new set by a scale factor called OPT scale factor. The new set of coefficients is then inverse transformed resulting in contrast improved image. Applications of the proposed method to mammograms with subtle lesions are shown. To validate the effectiveness of the proposed method, we compare the results to those obtained by the Histogram Equalization (HE) and the Unsharp Masking (UM) methods. Our preliminary results strongly suggest that the proposed method offers considerably improved enhancement capability over the HE and UM methods.

***Keywords*—**mammograms**,** image enhancement, orthogonal polynomials, contrast improvement

I. INTRODUCTION

BREAST cancer is one of the leading causes of women mortality in the world. The primary goal of mammography screening is to detect small, non-palpable cancers in its early stage. [1] But mammograms are difficult to interpret as the pathological changes of the breast are subtle and their visibility is poor in low contrast and noisy mammograms. In order to increase the visibility of features several algorithms for image enhancement are proposed in the literature. Image enhancement is an important step in Computer-Aided Detection (CADe) systems for automated analysis of mammograms. CADe systems have been developed to aid radiologists in detecting mammographic lesions that may indicate the presence of breast cancer. These systems act only as a second reader and the final decision is made by the radiologist. Some studies have shown that CADe systems, when used as an aid, have improved radiologists' accuracy for detecting breast cancer. Contrast enhancement is an essential technical aid in applications where human visual perception remains the primary approach to extract relevant information from images. A good number of studies have been carried out towards contrast improvement. R. M. Rangayyan et. al. [2] proposed an Adaptive Neighbourhood Contrast Enhancement (ANCE) technique for digitized mammograms in which objects are identified by a region-growing technique and selectively enhancing the visual contrast. The ANCE-processed mammograms increased the detectability of malignant signs at earlier stages as compared with the original and unprocessed digitized mammograms.

Enhancement in spatial domain results in enhancement of signal as well as noise. In order to overcome this limitation transformations to frequency domain were exploited by some research groups. The signal compression property of the transform allows separating signal from noise since signal energy is concentrated on a few large coefficients while noise energy is uniformly distributed among transform coefficients. This enables suppression of noisy coefficients (denoising) before contrast enhancement by thresholding the transform coefficients. P. Sakellaropulos et. al. [3] proposed a method for minimizing image noise while optimizing contrast of image features. This method is based on local modification of multi-scale gradient magnitude values provided by the redundant dyadic wavelet transform. A. Mencattini et. al. [4] proposed an algorithm for image denoising and enhancement based on dyadic wavelet processing. The denoising phase is based on local iterative noise variance estimation. Moreover, in the case of MCs, they proposed an adaptive tuning of enhancement degree at different wavelet scales, whereas in the case of mass detection, they developed a segmentation method combining dyadic wavelet information with mathematical morphology. The approach consists of using the same algorithmic core for processing images to detect both MCs and masses.

Frequently enhancement in digital radiography is interpreted as edge magnification for contrast enhancement. Several methods have been proposed by research groups for edge enhancement and method proposed by S. Dippel et. al. [5] amplifies the edges after removing low frequency contents of an image and retaining or amplifying high frequency components. The method utilizes Discrete Wavelet Transform for contrast enhancement of edge coefficients. J. Scharcanski

Dr. R. Krishnamoorthi is with the Computer Vision Lab, Bharathidasan Institute of Technology, Anna University, Tiruchirapalli, India – 620024; (email: rkrish07@hotmail.com)

N. Amudhavalli is with Division of Radiology & Imaging Sciences, Rajah Muthiah Medical College and Hospital, Annamalai University, Chidambaram, India – 608002; (corresponding author, email: namu71@gmail.com)

Dr. M. K. Sivakkolunthu is with Division of Radiology & Imaging Sciences, Rajah Muthiah Medical College and Hospital, Annamalai University, Chidambaram, India – 608002; (email: kolunthu@gmail.com)

et. al. [6] proposed another method for image denoising and edge enhancement using shift invariant redundant wavelet transform. The distribution of horizontal and vertical detail coefficients of wavelet transform is modeled by a composition of Gaussian and Laplacian probability density functions at each scale. Then the shrinkage functions are combined in consecutive levels to retain the edges and remove the residual noise. The denoised wavelet coefficients are adaptively enhanced to produce the edge enhanced image. M. Malfait et. al. [7] proposed a filter using Markov Random Field model involving Bayesian probabilistic framework for image denoising.

MC detection using fuzzy logic was proposed by H.D. Cheng et. al. [8] where the gray levels of an image were transformed to an interval [0, 1] using a function to locate the intensities of MCs. They employed fuzzy logic for transforming gray level contrast and local gray level variations into the fuzzy domain by creating a fuzzy image using low-pass filtering. In the fuzzy domain, the fuzziness of a content of interest is represented, and contrast enhancement and sharpening of details are performed in the fuzzy domain. The effect of an image enhancement processing stage and the parameter tuning of a CAD system for the detection of MCs in mammograms was assessed by A. Papadopoulos et. al. [9] Five image enhancement algorithms were tested introducing the contrast-limited adaptive histogram equalization (CLAHE), the local range modification (LRM), redundant discrete wavelet (RDW), linear stretching and shrinkage algorithms. P. Heinlein et. al. [10] proposed an algorithm for feature enhancement in mammograms using discrete wavelet decompositions, to enhance MCs. M. G. Linguraru et. al. [11] presented an algorithm for detecting MCs based on a biologically inspired contrast detection algorithm in combination with preprocessing steps which involved shot noise, Curved Linear Structure removal, image enhancement and image normalization. H. Li et. al. [12] proposed a fractal modeling scheme for the enhancement of MCs. The breast parenchymal structures result in high local self-similarity which is decreased by the presence of MCs. This property enables the MCs to be enhanced based on the difference between the original and the fractal modeled image. M. P. Sampat et. al. [13] proposed an approach for enhancement of spicules of spiculated masses using discrete radon transformation. The performance analysis of their method was carried out subjectively. The region of interest containing the spiculated mass was cropped and used for further analysis. Another method was proposed by A. R. Dominguez et. al. [14] for enhancement of masses that improves the image contrast based on statistical measures. The method was tested on 57 mammographic images containing masses. J. Tang et. al. [15] proposed an image enhancement algorithm for low vision patients by enhancing the images in the discrete cosine transform domain by weighting the quantization table in the decoder.

The medical images vary widely in terms of acquisition, noise characteristics and quality. Hence it necessitates to process on image by image basis. This motivates the design and construction of versatile denoising and enhancement method that is applicable to various circumstances. This paper presents an Orthogonal Polynomials based enhancement technique which enhances the subtle density differences of X - ray mammograms. The resulting output improves visual analysis and serves as a basis for the automatic quantification of the breast image analysis. In this work, we propose a new adaptive method for image denoising and enhancement, which combines detection, enhancement of edges that are hidden behind the dense textural region and shrinkage of textural noise. The detection of significant edges is carried out using statistical testing based on Bartlett's criteria with the OPT coefficients. The OPT is a widely used unitary transformation for image analysis and compression with software implementations [16, 17]. Although the utility of each OPT coefficient in pattern recognition has never been outlined in medical images, these coefficients are useful for image processing and signal enhancement. Indeed, OPT coefficients have potential to perform both basic and complex image processing operations. One such signal enhancement technique is investigated for X-ray mammograms.

The proposed approach is flexible enough to allow the user to select the desired image enhancement. Also, it does not require the user to alter any parameters for image denoising. This paper is organized as follows. In Sections II and III the proposed orthogonal polynomials transformation is presented. In Section IV, the proposed contrast enhancement technique using OPT scale factor upon edges and suppression of noise is described. The performance analysis used to evaluate the proposed technique is described in Section V. Finally, the experiments and results are discussed in Section VI.

II. Orthogonal Polynomials Transformation

A linear 2-D image formation system is usually considered around a Cartesian coordinate separable, blurring, point spread operator in which the image I results in the superposition of the point source of impulse weighted by the value of the object function f. Expressing the object function f in terms of derivatives of the image function I relative to its Cartesian coordinates is very useful for analyzing the image. The point spread function $M(x, y)$ can be considered to be real valued function defined for $(x, y) \in X$ x Y, where X and Y are ordered subsets of real values. In case of gray-level image of size (n x n) where X (rows) consists of a finite set, which for convenience can be labeled as {0, 1, …, n-1}, the function $M(x, y)$ reduces to a sequence of functions.

$$M(i,t) = u_i(t), i,t = 0,1,..., n-1 \quad (1)$$

The linear two dimensional transformation can be defined by the point spread operator $M(x,y)(M(i,t) = u_i(t))$ as shown in equation (2).

$$\beta(\zeta,\eta) = \int_{x\in X}\int_{y\in Y} M(\zeta,x)M(\eta,y)I(x,y)dxdy \quad (2)$$

where ζ, η are coordinates in the 2-D transformed space and

$I(x, y)$ is a mammogram image region wherein x and y are two spatial coordinates. Considering both X and Y to be a finite set of values {0, 1, 2 … n –1}, equation (2) can be written in matrix notation as follows

$$\left|\beta_{ij}^{'}\right| = \left(|M| \otimes |M|\right)^{t} |I| \tag{3}$$

where $\otimes$ is the outer product, $|\beta'_{ij}|$ and $|I|$ are n^2 matrices arranged in the dictionary sequence, $|I|$ is the image , $|\beta'_{ij}|$ are the coefficients of transformation and the point spread operator $|M|$ is

$$|M| = \begin{vmatrix} u_0(t_1) & u_1(t_1) & \cdots & u_{n-1}(t_1) \\ u_0(t_2) & u_1(t_2) & \cdots & u_{n-1}(t_2) \\ & \vdots & & \\ u_0(t_n) & u_1(t_n) & \cdots & u_{n-1}(t_n) \end{vmatrix} \tag{4}$$

We consider a set of orthogonal polynomials $u_0(t)$, $u_1(t)$, …, $u_{n-1}(t)$ of degrees 0, 1, 2, …, n-1 respectively to construct the polynomial operators of different sizes from equation (4) for n ≥ 2 and t_i = i. The generating formula for the polynomials is as follows.

$$\begin{aligned} &u_{i+1}(t) = (t-\mu)\, u_i(t) - b_i(n)\, u_{i-1}(t) \; for\; i \geq 1, \\ &u_1(t) = t-\mu \text{ and } u_0(t) = 1 \end{aligned} \tag{5}$$

$$\text{where } b_i(n) = \frac{i^2\left(n^2 - i^2\right)}{4\left(4i^2-1\right)}, \qquad \mu = \frac{1}{n}\sum_{t=1}^{n} t = \frac{n+1}{2}$$

We can construct point-spread operators $|M|$ of different size from equation (4) using the above orthogonal polynomials for $n \geq 2$ and $t_i = i$. For the convenience of point-spread operations, the elements of $|M|$ are scaled to make them integers.

III. The Orthogonal Polynomial Basis

For the sake of computational simplicity, the finite Cartesian coordinate set X, Y is labeled as {1, 2, 3}. The point spread operator in equation (3) that defines the linear orthogonal transformation for image can be obtained as $|M| \otimes |M|$, where $|M|$ can be computed and scaled from equation (4) as follows.

$$|M| = \begin{vmatrix} u_0(x_0) & u_1(x_0) & u_2(x_0) \\ u_0(x_1) & u_1(x_1) & u_2(x_1) \\ u_0(x_2) & u_1(x_2) & u_2(x_2) \end{vmatrix} = \begin{vmatrix} 1 & -1 & 1 \\ 1 & 0 & -2 \\ 1 & 1 & 1 \end{vmatrix} \tag{6}$$

The set of polynomial basis operators O_{ij}^{n} $(0 \leq i, j \leq \text{n-1})$ can be computed as

$$O_{ij}^{n} = \hat{u}_i \otimes \hat{u}_j^{t}$$

where $\hat{u}_i$ is the (i + 1) st column vector of $|M|$. The complete set of basis operators of sizes (2 X 2) is given below. Polynomial basis operators of size (2 * 2) are

$$\left[O_{00}^{2}\right] = \begin{bmatrix} 1 & 1 \\ 1 & 1 \end{bmatrix}, \quad \left[O_{01}^{2}\right] = \begin{bmatrix} -1 & 1 \\ -1 & 1 \end{bmatrix}, \quad \left[O_{10}^{2}\right] = \begin{bmatrix} -1 & -1 \\ 1 & 1 \end{bmatrix},$$

$$\left[O_{11}^{2}\right] = \begin{bmatrix} 1 & -1 \\ -1 & 1 \end{bmatrix}$$

Since the operator M, defined in equation (6) is orthogonal and complete, it is evident that the transformation (equation (3)) is complete and the reconstruction can be expressed as

$$\left[I_{i,j}^{3}\right] = \sum_{i=0}^{2}\sum_{j=0}^{2} \beta_{ij}\left[O_{i,j}^{3}\right] \tag{7}$$

where $|\beta| = \left(|M|^{t}|M|\right)^{-1}|\beta^{'}|\left(|M|^{t}|M|\right)^{-1}$, $\left[I_{i,j}^{3}\right]$ is the (3 X 3) gray level image matrix, $\left[O_{i,j}^{3}\right]$ accounts for the spatial, model variation and $|\beta_{i,j}|$ is the $(i, j)^{\text{th}}$ coefficient of variation. Having discussed the orthogonal polynomials model for the forward and inverse transformations, the proposed image enhancement technique is presented in the following section.

IV. Proposed Image Enhancement in the OPT Domain

A small mammographic image region which is a function of two spatial co-ordinates is represented by a set of orthogonal polynomials. In this representation, the image region is considered to be a linear combination of uncorrelated (orthogonal) effects due to spatial variations. The uncorrelated effects due to the presence of edge have been separated successfully from those due to the presence of textures. The presence of edge and texture in the image region under analysis is detected on the basis of the strength of the appropriate orthogonal effects. Consider a gray level image I(x, y) of size (R X C), where x, y are the two spatial coordinates. The function I(x, y) which represents the gray level of the pixel is considered as a random variable. Thus, I(x, y) can be expressed as

$$I(x, y) = g(x, y) + \eta(x, y) \tag{8}$$

where g(x, y) accounts for the spatial variation owing to edge in I(x, y) and ŋ(x, y) is the spatial variation owing to texture. In order to measure the spatial variations owing to edge and texture separately, we represent I(x, y) as shown in equation(7). In general, equation (7) can be represented as

$$\left[I_{i,j}^{n}\right] = \sum_{i=0}^{n-1}\sum_{j=0}^{n-1} \beta_{ij}\left[O_{i,j}^{n}\right] \tag{9}$$

where "n" stands for block size. It has been observed experimentally that the spatial variation that causes the interaction effects are owing to micro texture present in the mammogram image region $\left[I_{i,j}^{n}\right]$. The spatial variations g(x, y) and ŋ(x, y) can be approximated by an appropriate set of orthogonal functions. In this regard, a set of orthogonal polynomials have been discussed and the discrete formulation

has been used to determine a set of orthogonal effects, β'_{ij} due to the micro edge and micro texture. These effects are obtained from equation (3) and transformed matrix of block size (4 X 4) is represented as follows as this block size is used in our experiments:

$$\beta'_{ij} = [M]^t [I][M] = \begin{bmatrix} \beta'_{00} & \beta'_{01} & \beta'_{02} & \beta'_{03} \\ \beta'_{10} & \beta'_{11} & \beta'_{12} & \beta'_{13} \\ \beta'_{20} & \beta'_{21} & \beta'_{22} & \beta'_{23} \\ \beta'_{30} & \beta'_{31} & \beta'_{32} & \beta'_{33} \end{bmatrix} \quad (10)$$

where s at i = 0, 0 < j ≤ 3 and j = 0, 0 < i ≤ 3 are considered as responses towards edges and the remaining responses are assumed to be the responses towards textures as per grouping criteria proposed in [16]. Various micro textured regions can be characterized by estimating the orthogonal effects and their mean square variances. The mean square variances S_{ij}^2 s corresponding to the orthogonal effects β_{ij} s are computed as follows.

$$[\beta_{ij}] = ([M]^t [M])^{-1} ([M]^t [I][M])([M]^t [M])^{-1}) \quad (11)$$

$$[S_{ij}{}^2] = ([M]^t [M])^{-1} ([M]^t [I][M])^2 ([M]^t [M])^{-1}) \quad (12)$$

A. Statistical Testing for Selective Signals

The mean square variances are grouped in to two sets such that set $\psi_e = \{ S_{ij}^2 \}$, where i = 0, 0 < j ≤ 3 and j = 0, 0 < i ≤ 3, are the set of variances due to the main effects and set $\psi_t = \{ S_{ij}^2 \}$, where 0< i ≤ 3, 0 < j ≤ 3, are the set of variances due to the interaction effects. In order to test whether a given region belongs to a textured region, statistical testing based on Bartlett's [18] criteria for testing the homogeneity among the variances is carried out.

After deciding whether the block requires enhancement depending on the presence of significant edges compared to the texture present based on statistical testing, proposed contrast enhancement is carried out. The proposed contrast enhancement technique is discussed below.

B. Contrast Enhancement and Adaptive Denoising

Any real signal is corrupted by some noise. Any image contains a true signal and additional signals of no interest which can be termed as noises. Especially, in medical image, suppression of noise is a difficult task. In image denoising, one often faces uncertainty about the presence of a given "feature of interest" (e.g., an image edge) in the presence of noise. The enhancement operation should highlight the diagnostically relevant image features like edges in addition to denoising. In the proposed method, denoising refers to the suppression of textural features. Since, the presence of edge features are hidden by dense parenchymal patterns of mammograms, it is first necessary to denoise the data through the frequency components in the proposed OPT domain. However, conventional filtering techniques cannot be applied in the context of medical imaging because they produce edge blurring and loss of details. To achieve edge enhancement, we apply the novel OPT scale factor on the transformed coefficients of given in equation (11).Thus we have

$$\beta^*_{ij} = k^{i+j} \beta_{ij} \quad (13)$$

where i = 0, 0 < j ≤ 3 and j = 0, 0 < i ≤ 3 for coefficients that correspond to responses towards edges. β^*_{ij} is the scaled coefficient and k is OPT scale factor. In case of image block which is considered for enhancement as a result of statistical testing, the texture coefficients are assumed to be noises and they have to be suppressed. So, the corresponding texture coefficients are multiplied with OPT scale factor given in equation (14) as follows:

$$k^{i+j} = 0 \quad (14)$$

where 0< i ≤ 3, 0 < j ≤ 3 for coefficients that correspond to responses towards texture. Thus, the proposed scheme involves zeroing the coefficients corresponding to texture resulting in noise suppression and scaling of coefficients corresponding to edges by OPT scale factor.

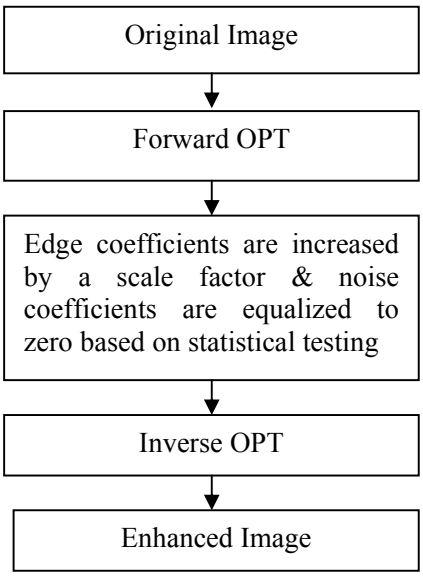

Fig. 1 Flowchart of proposed image enhancement in OPT domain

The signal compression property of the transform allows separating the signal from noise as the signal is concentrated on few transformed coefficients and this property of the transform is established in [17]. Then the modified OPT coefficients are inverse transformed. The inverse transformation is carried out using the orthogonal polynomial basis functions as given in section III. This inverse operation results in the enhancement of image edges depending on the selection of OPT scale factor. Fig. 1 shows the flow chart of the proposed image enhancement using the orthogonal

polynomials framework.

V. Performance Measure

A. Quantitative analysis

In order to measure the performance of the proposed contrast enhancement method, the Mammographic Image Analysis Society (MIAS) database of University of Essex, England consisting of digitized mammograms [19] is utilized. The dataset consisted of 322 medio-lateral oblique (MLO) mammograms and correspond to all density categories. The proposed OPT framework is applied on all 322 images of MIAS database.

In order to evaluate the quality of enhanced images quantitatively, contrast, calculated from the co-occurrence matrices of original and enhanced images is used as the metric for image enhancement. The co-occurrence method [20] is based on the repeated occurrence of some gray level configuration. In co-occurrence matrix, an occurrence of some gray level configuration was described by a matrix of relative frequencies *(i, j)*, describing how frequently two pixels with gray levels *i, j* appear in the image separated by a distance d = (*dx, dy*), where *dx* and *dy* represent the displacement in the x and y direction, respectively. In our implementation, the co-occurrence matrix *C*(*i, j*) is derived with distance d = (1, 1), i.e., one pixel below and one pixel right and contrast is calculated from the co-occurrence matrix using (15).

$$Contrast = \sum_{i,j=0}^{n-1} (i-j)^2 C(i,j) \quad (15)$$

where *C(i, j)* is the Grey Level Co-occurrence Matrix (GLCM).

B. Qualitative analysis

Three experienced radiologists ranked the performance of each original and the corresponding processed images of the sample (from 1 = best to 4 = worst) with respect to contrast and morphological (MC cluster characteristics such as number, shape, size, density; Mass characteristics such as center, contour, shape, size) characteristics of lesion. The sample is limited to fifty mammograms from MIAS database that includes all BIRADS (1 – 4) density categories with twenty five cases containing masses and twenty five cases containing MCs.

VI. Experiments and Results

The proposed denoising and image enhancement in OPT domain has been experimented with all 322 X-ray mammograms available from MIAS database. The X-ray mammograms are characterized with inherent noise. One such mammogram containing MC cluster is shown in fig. 2(a). The image is partitioned into overlapping (4 X 4) regions in a sliding window technique and are applied with OPT in each sub-image regions, as described in section II. The coefficients corresponding to edges and textures are grouped from the resulting transformation coefficients, according to statistical testing based on Bartlett's criteria, as described in section IV A. Then, the coefficients corresponding to edge features are adaptively enhanced by multiplying with OPT scale factor and the texture coefficients are suppressed as described in section IV B. Upon carrying out the bidirectional edge enhancement, the scaled coefficients are inverse transformed as explained in section III, resulting in edge enhanced and contrast improved mammogram image. The resulting output of the proposed image enhancement in OPT domain with scale factor $k = 2$ is shown in fig 2(b). The experiment is repeated for OPT scale factors 3, 4, 5 and 6 and the resulting outputs are shown in fig. 2(c), 2(d), 2(e) and 2(f) respectively. The corresponding GLCM contrast measures as calculated from equation (16) are 63.93, 75.05, 84.99, 96.36 and 109.24 compared to 31.46, which is obtained for original image 2(a).

To evaluate image enhancement quality we have used GLCM contrast measure as a means of quantitative assessment of the different contrast enhancement methods presented in this paper. In order to evaluate the effectiveness of the proposed enhancement technique against other commonly used contrast enhancement methods, twelve randomly selected mammograms from MIAS database are considered. The GLCM contrast measure values obtained for OPT scale factor 1, 2, 3, 4, 5 and 6 for 12 mammogram images are presented in Table I. The OPT scale factor equal to 1 represents the original mammogram as there is no scaling of transformed coefficients. As expected, increase of the OPT scale factor results in increase of contrast measure.

The scale factor k can be adjusted by the user and the desired degree of enhancement can be selected. The adjustment is left to the medical expert who finally controls the image interpretation. Increasing the scale factor leads to an increased smoothing of weak image textures while enhancing the presence of the main image discontinuities, as shown in fig. 2(b) to 2(f). It can be seen from the images that scale factors ranging from 4 to 6 are adequate for which the presence of microcalcifications are distinctly visible. The results demonstrate that the increase of OPT scale factor leads to a stronger suppression of the background texture and to the enhancement of sharp intensity variations.

Also, four sample images viz. image containing minute MC cluster, MC cluster, spiculated lesion and well circumscribed mass, with pixel values in the range 0 - 255 are shown in fig 3(a) , 4(a) , 5(a), 6(a), respectively. The resulting output of the proposed enhancement in OPT domain are shown in fig 3(b), 4(b), 5(b), 6(b), respectively. In each case, the OPT scale factor used equals to five. The enhanced images are analyzed quantitatively (contrast measure of the enhanced image) and qualitatively (visual estimates). In this study, experimental results from proposed enhancement method are compared with two conventional methods of image enhancement such as histogram equalization and unsharp masking. The histogram equalization enhances each pixel based on the histogram equalization of pixels within a region (i.e., a moving window) surrounding the pixel. In this experiment, the size of the moving window is (64 X 64)

pixels. The unsharp masking adds the gradient value weighted by the contrast gain to the original image. A commonly used gradient function is the Laplacian operator. In this experiment, the contrast gain has a value of five. Eventhough different degrees of enhancement could be used, in order to compare the result constant gain factor is used. The GLCM Contrast values C_{ORIG} for original mammogram, C_{HE} for enhancement by histogram equalization, C_{UM} for enhancement by unsharp masking, C_{OPT} for enhancement by proposed method using OPT are calculated and given in Table II. It is evident from the Table II that the proposed method achieves higher contrast measure compared to histogram equalization and unsharp masking.

According to radiologists qualitative analysis, the proposed method has shown promising results in enhancing visibility of lesions against dense parenchymal background. The proposed method demonstrates the highest performance in both lesion types. The histogram equalization method fails in visualizing both masses and MCs which is evident from the visual analysis of the images considered in fig. 3, Fig. 4. Fig. 5 and fig. 6.

The average rank obtained from the three experienced radiologists, for original and the three image enhancement methods are obtained as described in section VB. The radiologists ratings with respect to contrast and morphology of lesions is presented in fig. 7 and fig. 8 respectively. A low rank indicates a high preference. Reported results indicate that edge enhancement based on contrast improvement in OPT domain facilitates the interpretation of mammograms. In the enhanced mammogram image, both retro mammary fat plane and mammary gland are clearly visualized. The areola, skin, subcutaneous fat, surface veins and some of the peripheral cooper's ligaments are better visualized than in the original mammographic image according to radiologist's opinion.

VII. Conclusion

The presented results confirm the usefulness of OPT based processing methods for improving mass and MC detection and improved visualization of peripheral structures. This testifies the superiority of the enhanced mammograms over the original mammograms in several cases. The scale factor often enable better edge enhancement but in some cases result in over enhancement. We noticed exciting clear indications of mass and MC detection with undoubted interpretation. Nevertheless, image enhancement in OPT domain seems to be useful and more promising. According to the opinion of radiologists who participated in the qualitative analysis, the proposed 'enhanced view' would be particularly useful when enhanced images are displayed together with original mammograms. Intensification of density distinctions due to significantly increased local contrast resolution should be interpreted and utilized as a supplement to conventional display. Contrast enhancement can assist radiogist's interpretation of an image and in addition can facilitate the automated interpretation. Thus, the proposed technique is suitable for visually meaningful segmentation of masses and microcalcifications for automated analysis of mammograms. It is a transform domain technique and thus it can be easily integrated with the existing image coding standards such as JPEG, JPEG 2000. It is reported that the proposed technique is able to obtain more robust characteristics for noise suppression and detail preservation. The proposed method is of low complexity, as the transform involves integer values.

References

[1] S. A. Feig, "Decreased cancer mortality through mammographic screening: Results of clinical trials", *Radiology*, vol. 167, pp. 659-665, 1988.

[2] R. M. Rangayyan, L. Shen, Y. Shen, J. E. L. Desautels, H. Byrant, T. J. Terry, N. Horeczko, and M. S. Rose, "Improvement of sensitivity of breast cancer diagnosis with adaptive neighborhood contrast enhancement of mammograms", *IEEE Trans. Inf. Technol. Biomed.*, vol. 1, no. 3, pp. 161–169, 1997.

[3] P. Sakellaropulos, L. Costaridou and G. Panayiotakis, "A wavelet-based spatially adaptive method for mammographic contrast enhancement," *Physics in Medicine and Biology*, vol. 48, no. 6, pp.787-803, 2003.

[4] A. Mencattini, M. Salmeri, R. Lojacono, M. Frigerio, and F. Caselli, "Mammographic Images Enhancement and Denoising for Breast Cancer Detection Using Dyadic Wavelet Processing", *IEEE Trans. Inst. and Meas.*, vol. 57, no. 7, pp. 1422-1430, 2008.

[5] S. Dippel, M. Stahl, R. Wiemker, and T. Blaffert, "Multiscale Contrast Enhancement for Radiographies: Laplacian Pyramid Versus Fast Wavelet Transform", *IEEE Trans. Med. Imaging,* vol. 21, pp. 343 – 353, 2002.

[6] J. Scharcanski and C. Jung, "Denoising and enhancing digital mammographic images for visual screening", *Comput Med Imaging Graph*., vol. 30, no. 4, pp. 243-54, 2006.

[7] M. Malfait and D. Roose, "Wavelet based image denoising using a Markov Random Field a priori model*", IEEE Trans. Image Processing*, vol. 6, no. 4, pp. 549–565, 1997.

[8] H.D. Cheng and H. Xu, "A novel fuzzy logic approach to mammogram contrast enhancement", *Information Sciences*, vol. 148, pp. 167-184, 2002.

[9] A. Papadopoulos, D.I. Fotiadis and L. Costaridou, "Improvement of microcalcification cluster detection in mammography utilizing image enhancement techniques", *Computers in Biology and Medicine*, vol. 38, pp. 1045 – 1055, 2008.

[10] P. Heinlein, J. Drexl and W. Schneider, "Integrated wavelets for enhancement of microcalcifications in digital mammography", *IEEE Trans. Medical Imaging*, vol. 22, pp. 402–413, 2003.

[11] M. G. Linguraru, K. Marias, R. English and M. Brady, "A biologically inspired algorithm for microcalcification cluster detection", *Medical Image Analysis*, vol. 10, pp. 850–862, 2006.

[12] H. Li, K.J.U. Liu and S.C.B. Lo, Fractal modeling and segmentation for the enhancement of microcalcifications in digital mammograms, *IEEE Trans. Med. Imaging*, vol. 16, no.6, pp. 785–798, 1997.

[13] M. P. Sampat, G. J. Whitman, A. C. Bovik and M. K. Markey, "Comparison of Algorithms to Enhance Spicules of Spiculated Masses on Mammography", *Journal of Digital Imaging*, vol. 21, no. 1, pp. 9- 17, 2008.

[14] A. R. Dominguez and A. K. Nandi, "Detection of masses in mammograms via statistically based enhancement, multilevel-thresholding segmentation, and region selection", *Comp. Med. Imaging and Graph.*, vol. 32 pp. 304–315, 2008.

[15] J. Tang and E. Peli, "An Image Enhancement Algorithm in JPEG Domain for Low-vision Patient", *IEEE Transaction On Biomedical Engineering*, vol. 51, no.11, pp. 2013- 2023, 2004.

[16] L. Ganesan and P. Bhattacharyya, "Edge Detection in Untextured and Textured Images-A Common Computational Framework**",** *IEEE Trans. Syst. Man Cybern,* vol. 27, no. 5 pp. 823-834, 1997.

[17] R. Krishnamoorthi, "Transform coding of monochrome images with a statistical design of experiments approach to separate noise", *Pattern Recognition Letters*, vol. 28 , pp. 771–777, 2007.

[18] M. S. Bartlett, "Properties of sufficiency and statistical tests", *Proceedings of the Royal Statistical Society Series A*, vol. 160, pp. 268–282, 1937.
[19] J. Suckling, J. Parker, D. R. Dance, S. Astley, I. Hutt, C. R. M. Boggis, I. Ricketts, E. Stamatakis, N. Cerneaz, S. L. Kok, P. Taylor, D. Betal, and J. Savage, "The mammographic image analysis society mammogram database," in Proc. 2nd Int. Workshop Digital Mammography, York, U.K., pp. 375–378, 1994.
[20] R. M. Haralick, K. Shanmugan and I. Dinstein, "Textural features for image classification", *IEEE Trans. On Systems, Man and Cybernetics*, vol. 3, pp. 610-621, 1973.

TABLE I
CONTRAST MEASURE FOR DIFFERENT OPT SCALE FACTOR (k)

Image no.	k=1	k=2	k=3	k=4	k=5	k=6
mdb015	31.39	51.05	59.16	70.57	85.08	102.55
mdb025	27.90	30.58	39.39	59.47	80.56	96.48
mdb028	28.01	34.01	36.62	42.32	50.23	60.84
mdb198	50.39	66.09	81.58	107.37	125.79	143.02
mdb199	35.74	62.09	69.44	79.77	92.50	107.80
mdb209	35.42	56.98	83.27	113.52	138.86	164.70
mdb211	33.22	56.78	63.17	72.44	83.85	97.59
mdb222	27.40	34.88	45.74	64.39	86.12	106.04
mdb223	22.29	46.84	58.47	70.65	83.88	98.57
mdb245	31.45	63.92	75.07	84.98	96.35	109.23
mdb271	25.85	30.63	42.25	65.28	90.55	110.60
mdb290	30.53	31.71	33.64	41.05	53.34	70.91

TABLE II
CONTRAST VALUES C_{ORIG} FOR ORIGINAL MAMMOGRAM, C_{HE} FOR ENHANCEMENT BY HISTOGRAM EQUALIZATION, C_{UM} FOR ENHANCEMENT BY UNSHARP MASKING, C_{OPT} FOR ENHANCEMENT BY ADAPTIVE METHOD USING ORTHOGONAL POLYNOMIALS TRANSFORMATION

Image no.	C_{ORIG}	C_{HE}	C_{UM}	C_{OPT}
mdb015	31.39	48.78	71.48	102.55
mdb025	27.90	52.03	46.64	96.48
mdb028	28.01	51.73	58.44	60.84
mdb198	50.39	59.83	84.50	143.02
mdb199	35.74	51.49	100.41	107.80
mdb209	35.42	59.48	68.23	164.70
mdb211	33.22	43.60	92.60	97.59
mdb222	27.40	42.65	52.26	106.04
mdb223	22.29	64.49	50.71	98.57
mdb245	31.45	41.77	60.75	109.23
mdb271	25.85	49.97	45.93	110.60
mdb290	30.53	52.25	53.82	70.91

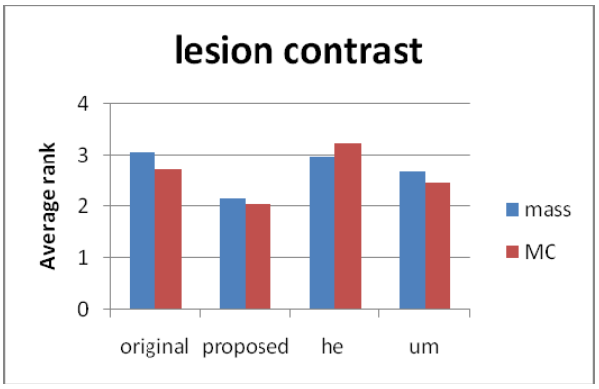

Fig. 7 Average rank for original and the three image enhancement methods with respect to lesion contrast

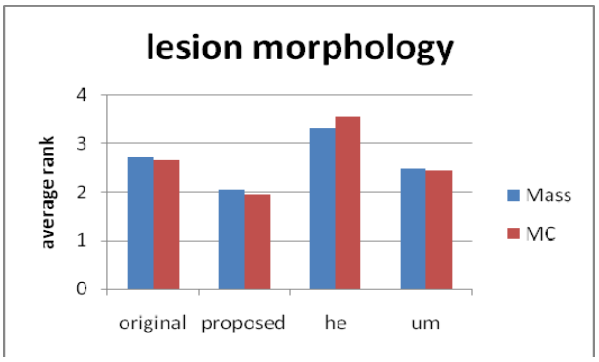

Fig. 8 Average rank for original and the three image enhancement methods with respect to lesion morphology

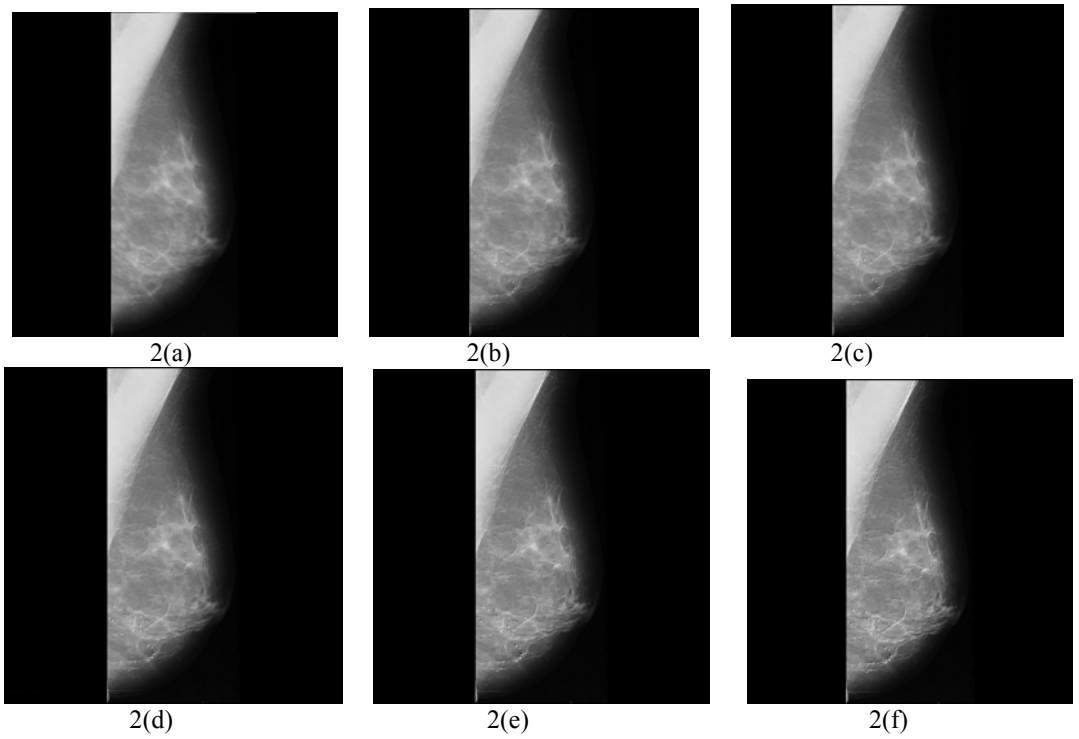

Fig. 2 (a) original mammogram (b) enhanced mammogram with OPT scale factor $k = 2$ (c) enhanced mammogram with $k = 3$ (d) enhanced mammogram with $k = 4$ (e) enhanced mammogram with $k = 5$ (f) enhanced mammogram with $k = 6$

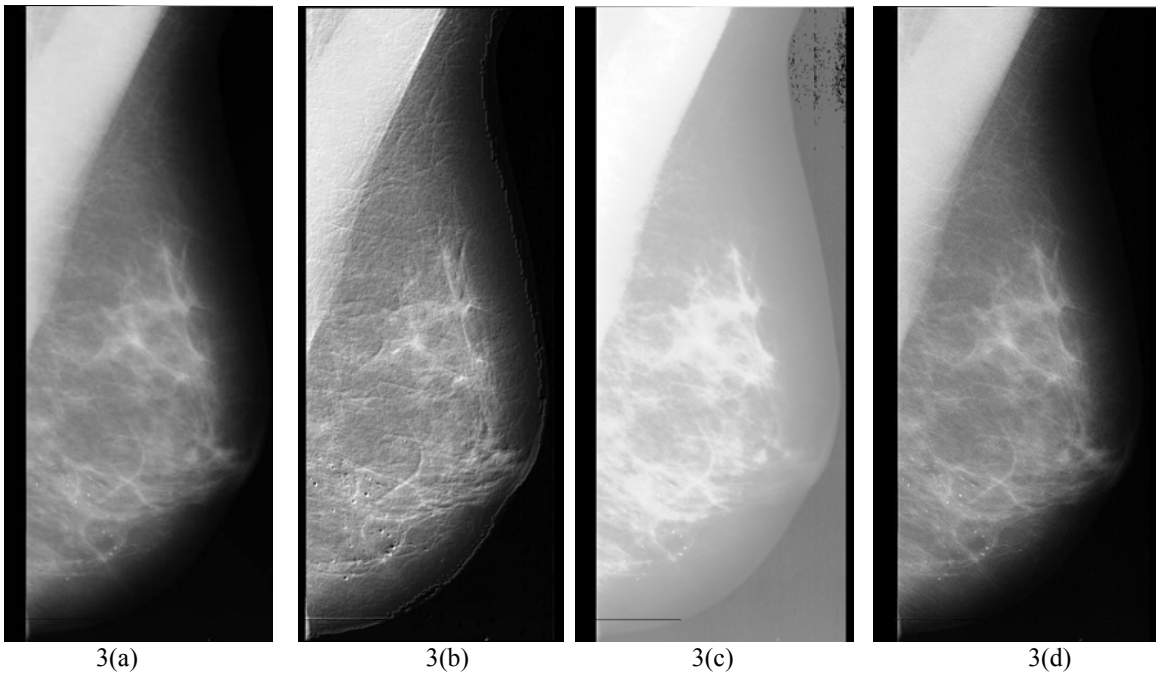

Fig. 3 (a) original mammogram containing MC cluster (b) image enhanced using proposed approach (c) Histogram Equalization of original image (d) Unsharp Masking of the original image

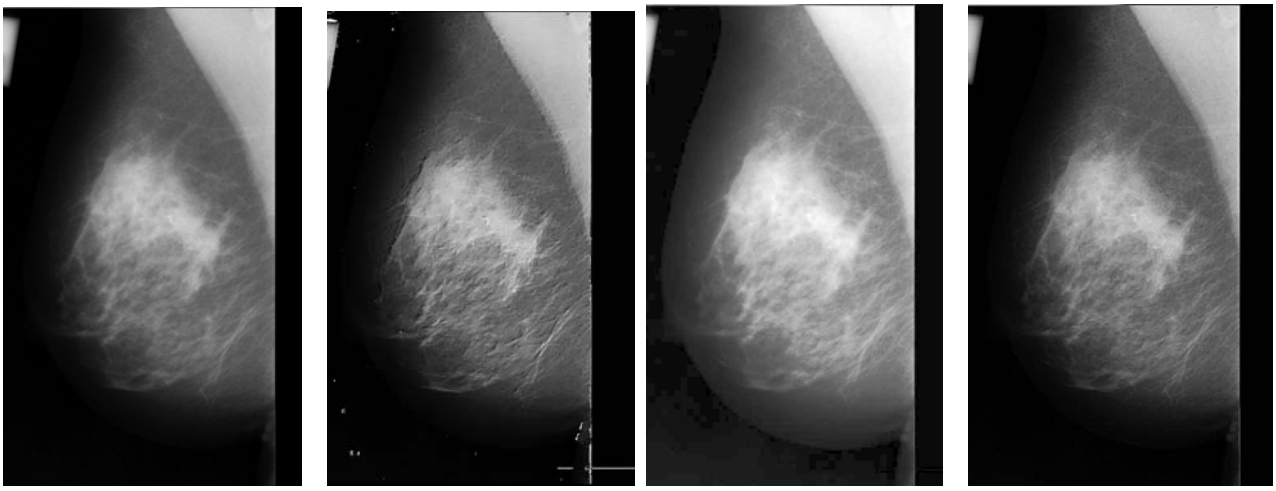

Fig. 4 Comparative results for the MIAS database mammogram 209, containing a MC clusters which is not clearly visible in denser areas (a) original image; (b) image enhanced using proposed approach (c) Histogram Equalization of original image (d) Unsharp Masking of original image

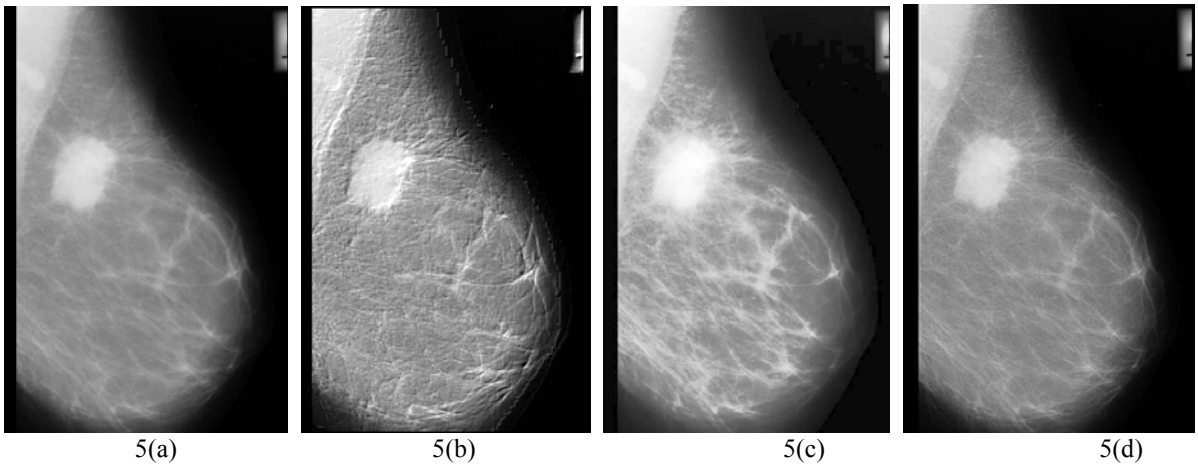

Fig. 5 (a) original mammogram containing spiculated mass (b) image enhanced by proposed approach (c) Histogram Equalization of original image (d) Unsharp Masking of original image

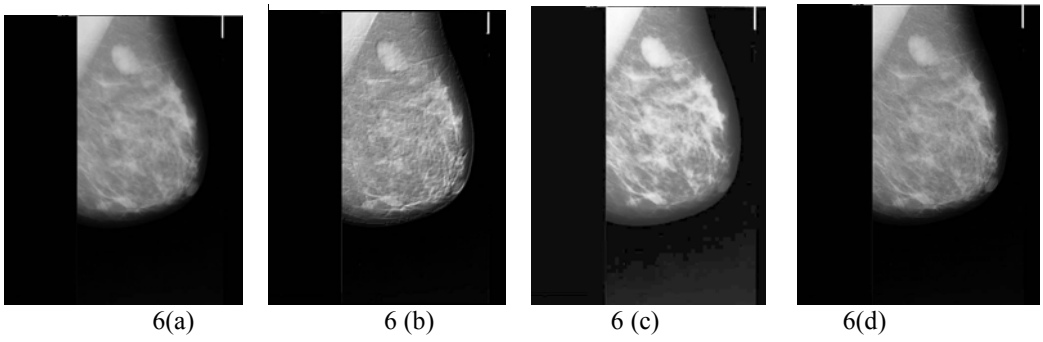

Fig. 6 (a) original mammogram containing mass (b) image enhanced by proposed approach (c) Histogram Equalization of original image (d) Unsharp Masking of original image